

# INITIAL VERIFICATION FOR THE ZY-3 SATELLITE POST-PROCESSING ATTITUDE ACCURACY

Junfeng XIE<sup>a</sup>, Xinming TANG<sup>a</sup>, Xiao WANG<sup>b\*</sup>, Sheng WANG<sup>c</sup>, Hunxue HUANG<sup>a</sup>

<sup>a</sup>SASMAC, Satellite Surveying and Mapping Application Center, NASG-junfeng\_xie@163.com

<sup>b</sup>Institute of Remote Sensing and Digital Earth Chinese Academy of Sciences, China-  
wangxiao@radi.ac.cn

<sup>c</sup>State key Laboratory of Information Engineering in Surveying, Mapping and Remote Sensing, Wuhan  
University

**ABSTRACT:** Attitude accuracy is one of the key factors that influence satellite mapping accuracy. By use of the raw data of the star tracker and the inertial gyro downloaded from ZY-3 satellite, the Forward-Backward smoothing filter with Unscented Kalman Filter (UKF) is applied and implemented for attitude post-processing to improve the attitude accuracy of ZY3 satellite in this paper. The experiments for comparing with on-board attitude with the geometric positioning accuracy without ground control points (GCPs) are implemented. The result indicates that the post-processing attitude accuracy has achieved a better level than the on-board processing.

**KEYWORDS:** Attitude Accuracy, Star Tracker/gyro, Post-Processing, Geometric positioning accuracy

## 1. INTRODUCTION

With the rapid development of remote sensing satellite imaging technology satellite mapping has become an important way to access geospatial information. Many countries have launched or are developing mapping satellites. On March 2008, the State Council of China approved to develop China's first domestic civil high-resolution stereo mapping satellite. ZY-3 satellite is equipped with three panchromatic cameras (Forward, Nadir, and Backward) and one multispectral camera (red, green, blue, four near-infrared band), with the resolutions of 3.5, 2.1, 3.5, and 5.8 meters. The three panchromatic cameras forms a triple linear array for stereo mapping. The main mission is used for 1:50,000 and 1:25,000 topographic mapping and revision of China.

The stereo mapping accuracy is an important indicator to evaluate the performance of mapping satellite, especially the direct positioning accuracy and the stereo mapping accuracy of remote sensing images in the absence of GCPs. To ensure the mission can achieve the design goal, ZY-3 satellite equipped three star trackers (two ASTRO-10 star trackers and one domestic APS star tracker), three group inertial gyros and earth infrared trackers, et al. The attitude control on-board mainly uses star tracker/gyro combination mode to get high-precision attitude, but it still was limited by the computing and storage resources on orbit, so attitude determination precision can be improved further. Therefore, the raw attitude data of the star tracker and gyro are downloaded from the ZY-3 satellite firstly, which can back up attitude result on-board with each other to enhance the reliability of mapping production, and meanwhile used for attitude post-processing on the ground to further improve the attitude accuracy.

As real time requirement for on-orbit processing, the error model design of the attitude filtering is not complete, so filtering process is relatively simple and accuracy is not optimal. A new star tracker/gyro process filtering algorithm is designed and applied for attitude post-processing in this paper. Finally, the ground control data were used to verify and analyze

the accuracy, then evaluated the effectiveness of post-processing attitude.

## 2. COMBINATION ATTITUDE DETERMINATION STRATEGY

Based on the analysis of the various error sources affecting satellite attitude precision, the combined high-precision attitude determination system is established. The stellar images of domestic star tracker, and meanwhile, quaternion data measured by star tracker and gyro data on orbit can be processed on the ground through this system. The satellite attitude of inertial frame can acquired by this system using post-processing, which ensures the direct positioning accuracy can reach mapping accuracy requirement in the absence of GCPs.

The technique process is shown as Figure 1. It mainly include identification and rejection of the telemetry data outliers, accurately calibration of relative installation between star tracker and gyro, combination attitude determination based on proposed filtering, high-precision process of raw stellar image of domestic star tracker and so on. The star tracker and inertial gyro data processing based on forward-backward smoothing filter with UKF is most important. Based on all above, the post-processing software for the raw star tracker/ gyro attitude data was completed, which can directly service for ZY-3 satellite application system construction after test and verification.

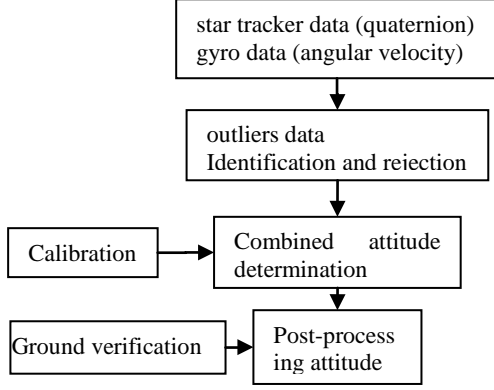


Fig. 1. Post-processing technical process

## 2.1 Unpack and Pre-process of Star Tracker/Gyro Data

Since signal transmission and reception, frames drop occasionally appear. For the raw star tracker/gyro data in binary format, it is necessary to unpack the data of star tracker (q value) and gyro angular velocity data firstly, based on which, the unpacked data are pre-processed. The outliers of the star tracker and the gyro due to transmission channel or accidental errors can be removed, so that the filter can be prevented divergent in the processing of the entire attitude calculation.

## 2.2 Combined Attitude Determination of Star Tracker/Gyro

### 2.2.1 Error Model Construction

For the on-board error model, a more sophisticated error measurement model by adding optical parameters of star tracker camera, gyro calibration parameters, and relative installation and so on is founded. This model is joined in UKF filter to improve the attitude filter accuracy. The strategies are shown in Figure 2.

The measure equation of gyro:

$$w_{gm} = w - b - \eta_a, \quad \dot{b} = \eta_r$$

$w_{gm}$  denotes the observation value in the inertial system.  $w$  denotes real angular velocity.  $b$  denotes gyro drift.  $\eta_a$  denotes random drift noise.

The attitude kinematics equation:

$$\dot{q} = \frac{1}{2}\Omega(w)q = \frac{1}{2}q \otimes \tilde{w}, \quad \delta q = q \otimes \hat{q}$$

It is linearized by differential as below:

$$\frac{d\delta q_v}{dt} = -\hat{w} \times \delta q_v + \frac{1}{2}\delta b + \frac{1}{2}\eta_a, \quad \frac{d\delta q_s}{dt} = 0$$

The superscript  $\hat{\quad}$  denotes the estimated value.  $\delta q_v$ ,  $\delta q_s$  denotes the scalar and vector quaternion deviation. The  $x = [\delta q_v, \delta b]$  denotes the system state vector, and the state equation is:

$$\frac{d}{dt} \begin{bmatrix} \delta q_v \\ \delta b \end{bmatrix} = \begin{bmatrix} -\hat{w} & \frac{1}{2}I \\ 0 & 0 \end{bmatrix} \begin{bmatrix} \delta q_v \\ \delta b \end{bmatrix} + \begin{bmatrix} \frac{1}{2}I & 0 \\ 0 & I \end{bmatrix} \begin{bmatrix} \eta_a \\ \eta_r \end{bmatrix}$$

If the vector part of quaternion deviation of star tracker is used as output of the observation equation, the expression of the observation equation is:

$$\delta q_{v,k+1} = H_{k+1} \begin{bmatrix} \delta q_v \\ \delta b \end{bmatrix}_{k+1} + v_{k+1}$$

In which,  $H_{k+1} = \begin{bmatrix} I_{3 \times 3} & 0_{3 \times 3} \end{bmatrix}$ ,  $v(k)$  denotes the measurement noise,  $E[v(k)] = 0$ ,  $E[v(k)v^T(j)] = R_k \delta_{k,j}$ ,  $R_k$  denotes the covariance matrix of measuring noise.

The initial state  $\mathbf{x}_0$  and the initial variance  $\mathbf{P}_0$  are given, according to state equation and measurement equation, the basic steps of UKF algorithm to estimate satellite attitude are as follows [1, 2, 3, 4]:

(1) Initialization:

$$\hat{\mathbf{x}}_0 = E[\mathbf{x}_0], \quad \mathbf{P}_0 = E[(\mathbf{x}_0 - \hat{\mathbf{x}}_0)(\mathbf{x}_0 - \hat{\mathbf{x}}_0)^T] \quad (a)$$

(2) Calculate sampling points and corresponding weights:

State dimensions  $n = 7$ ,  $2n+1$  sampling points and corresponding weights are calculated,  $k \geq 1$  and  $i = 1, 2, \dots, n$ .

$$\chi_{k-1} = [\hat{\mathbf{x}}_{k-1}, \hat{\mathbf{x}}_{k-1} + \sqrt{n+\tau}(\sqrt{\mathbf{P}_{k-1}}), \hat{\mathbf{x}}_{k-1} - \sqrt{n+\tau}(\sqrt{\mathbf{P}_{k-1}})] \quad (b)$$

$$W_{m0} = \tau/(n+\tau), \quad W_{c0} = \tau/(n+\tau) + 1 - \alpha^2 + \beta \quad (c)$$

$$W_{mi} = 1/[2(n+\tau)], \quad W_{mi+n} = 1/[2(n+\tau)] \quad (d)$$

$$W_{ci} = 1/[2(n+\tau)], \quad W_{ci+n} = 1/[2(n+\tau)] \quad (e)$$

$W_{mi}$  and  $W_{ci}$  are weighting factors of the mean value and variance of state parameters  $\mathbf{x}$ ;  $\alpha$  determines the distribution of the sampling points around the state mean. Little positive definite values  $0 \leq \alpha \leq 1$  are usually selected to avoid the sampling point nonlocal effects when do nonlinearity of equation of state,  $\beta$  is the parameter related with state prior distribution information, and it is non-negative weights,  $\beta \geq 0$ . When the sensor and the system noise is Gaussian distribution,  $\beta = 2$  is optimal, otherwise it is determined by simulation experiment,  $\tau$  is the scalar parameter, when state variable is single variable,  $\tau = \alpha^2(n+2) - n$ , when state variable is multivariable,  $\tau = 3\alpha^2 - n$ .

(2) Time update:

$$\chi_{k/k-1} = f(\chi_{k-1}, k-1), \quad \hat{\mathbf{x}}_k^- = \sum_{i=0}^{2n} W_{mi} \chi_{i,k/k-1} \quad (f)$$

$$\mathbf{P}_k^- = \sum W_{ci} [\chi_{i,k/k-1} - \hat{\mathbf{x}}_k^-][\chi_{i,k/k-1} - \hat{\mathbf{x}}_k^-]^T + \mathbf{Q}_k \quad (g)$$

$$y_{k/k-1} = H(\chi_{k/k-1}, k), \quad \hat{y}_k^- = \sum_{i=0}^{2n} W_{mi} y_{i,k/k-1} \quad (h)$$

$f(\chi_{k-1}, k-1)$  is discrete function of  $\mathbf{F}(X)$ .

(3) Measurement update:

$$P_{\hat{y}_k, \hat{y}_k} = \sum_{i=0}^{2n} W_{ci} [y_{i,k/k-1} - \hat{y}_k^-][y_{i,k/k-1} - \hat{y}_k^-]^T + \mathbf{R}_k \quad (i)$$

$$P_{x_k, y_k} = \sum_{i=0}^{2n} W_{ci} [\chi_{i,k/k-1} - \hat{\mathbf{x}}_k^-][y_{i,k/k-1} - \hat{y}_k^-]^T \quad (j)$$

$$\mathbf{K}_k = P_{x_k, y_k} P_{\hat{y}_k, \hat{y}_k}^{-1} \quad (k)$$

$$\hat{\mathbf{x}}_k = \hat{\mathbf{x}}_k^- + \mathbf{K}_k (y_k - \hat{y}_k^-) \quad (l)$$

$$\mathbf{P}_k = \mathbf{P}_k^- - \mathbf{K}_k P_{\hat{y}_k, \hat{y}_k} \mathbf{K}_k^T \quad (m)$$

In equation (g), (i),  $\mathbf{Q}_k$  and  $\mathbf{R}_k$  are state and measurement noise covariance matrix.

The optimal attitude quaternion and gyro drift can be estimated by UKF, and then the estimated attitude quaternion is normalized.

### 2.2.3 Filtering strategy

Based on all observational data accumulated for some time, the Forward-Backward filtering strategy is applied to obtain global optimum filtering results [5, 6, 7, 8, 9]. This strategy uses two-direction iterative method, each filtering process includes a forward UKF filtering and backward UKF filtering and smoothing with a weighted covariance. In the process of forward filtering, an attitude estimation error is introduced into error covariance matrix. Once the initial conditions of UKF filter are determined, the star tracker / gyro observations are updated to make the gain of UKF optimal, and the covariance matrix of this filtering is recorded. In the process of backward filtering, the weight can be determined by the forward and backward covariance, and the observed value can be smoothed in the reverse direction, and the final optimal result can be obtained by iteratively and repeated estimation. The process of smoothing filter is completed, which is shown as figure 2, 3.

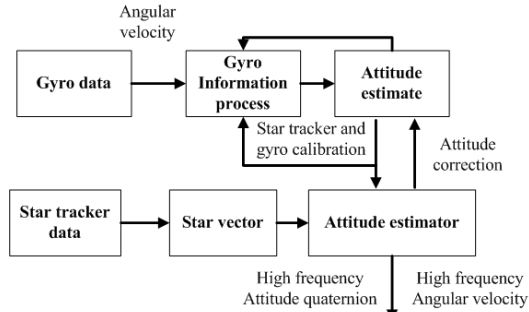


Fig. 2. Integrated attitude determination process

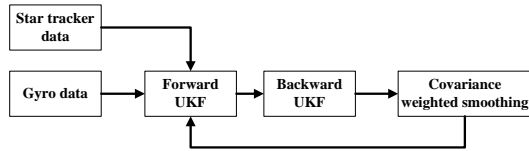


Fig. 3. Post global filtering strategy

## 3. Experiment and Analysis

### 3.1 Data Preparation

In the process of unpacking raw data, attitude data that dropped frames can be removed through checksum. The parameters of the camera and the star tracker/gyro were calibrated in the laboratory before launch, which were provided by satellite manufacturers. However, these parameters are required to be calibrated periodically on orbit, and based on which, the attitude accuracy can be estimated using direct positioning without GCPs.

According to coverage of existing GCPs, the satellite data covering Taiyuan region on the 457th track are selected for external parameters calibration, based on which, the data covering Tianjin region on the 785th track are chose to assess attitude accuracy with the GCPs.

The distribution of four GCPs on the strip image (six scenes) is shown as Figure 4.

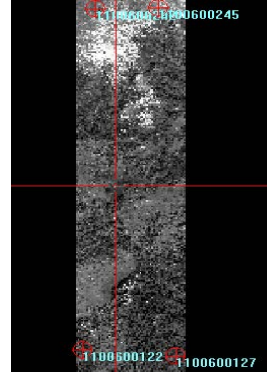


Fig. 4. The distribution of control points in Taiyuan

The single scene image covering Tianjin region is shown as Figure 5. The area was about 50km×50km. 10 GCPs were used as check points to check positioning accuracy without GCPs, and the three views(FWD ,NAD,BWD) are overlapped. The GPS were obtained by Continuously Operating Reference System (CORS), and the measuring accuracy is 3-5cm. The image coordinates of these GCPs are got by artificial prick.

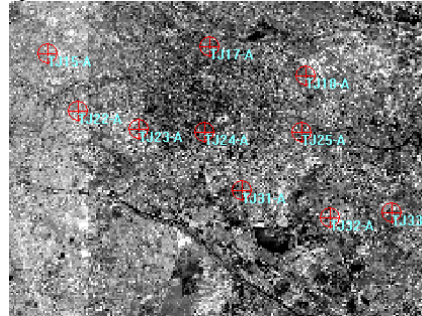


Fig 5. The distribution of control points in Tianjin

### 3.2 Attitude Post-Processing

After pre-processing of the original data of the 457th track (February 8, 2012) and the 785th track (February 28, 2012), attitude post-processing is implemented. In the process of integrated attitude determination, two star trackers can provide accurate absolute three-axis attitude. Compared with two floated gyro and domestic optical fiber gyro, the accuracy of three floated gyro was better. Three three-floated gyros and two star trackers are selected and integrated for absolute attitude determination. The post-processing attitude was obtained.

The absolute post-processing attitude by the unidirectional filtering and the bidirectional filtering changes with time are shown as Figure 6,7, and also the variation tendency of estimated gyro drift are shown as Figure 8,9.

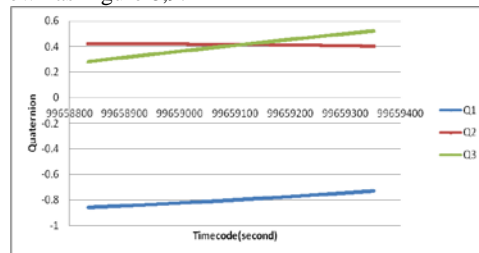


Fig. 6.The unidirectional filtering result (Quaternion)

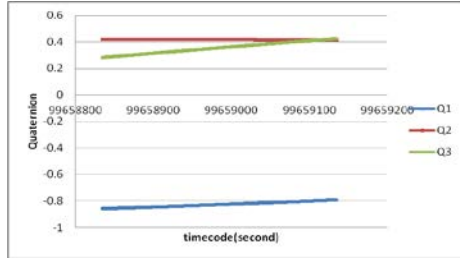


Fig 7. The bidirectional filtering result (Quaternion)

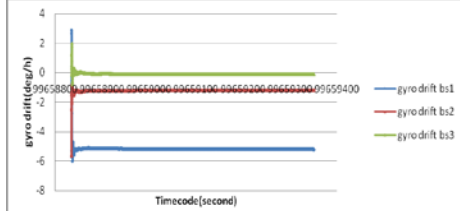


Fig 8. Gyro drift calibration (unidirectional filtering)

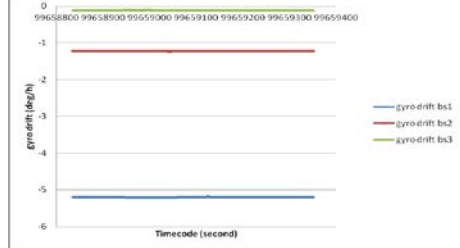


Fig 9. Gyro drift calibration (bidirectional filtering)

The error quaternion is obtained by comparing post-processing quaternion with on-board quaternion, and were converted into three-axis attitude error, which is shown as Figure 10, 11.

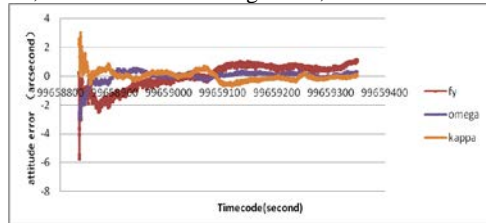


Fig 10. The attitude error (unidirectional filtering)

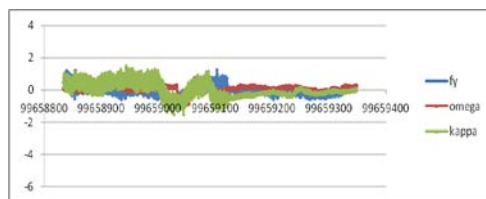


Fig 11. The attitude error (bidirectional filtering)

As seen in figure 6-11, the horizontal axis denotes the sample time, which is accumulated from January 1, 2009, and the unit is second. The variation of the gyro drift and attitude error using the unidirectional and bidirectional filtering with time is different. The result with the bidirectional filtering is more stable, which avoid the initial jitter. Meanwhile, the attitude random error is less than two arc seconds,

## 6. REFERENCE

[1]. Julier, S. J., 2002. The scaled unscented transformation, in: Proceedings of the American

Control Conference, Anchorage, USA, and 4555-4559.

## 3.3 Positioning Accuracy Analysis

The data covering Taiyuan region on the 457th track are used for external parameters including attitude systematic correction. Based on it, the single scene image on the 785th is employed to evaluate the geometric positioning accuracy without GCPs. 10 GCPs are applied as check points, and the verification results were shown in table 1.

| Three direction | Attitude type     | Min (m) | Max (m) | RMSE (m) |
|-----------------|-------------------|---------|---------|----------|
| X               | on-board attitude | -2.734  | -7.338  | 5.296    |
|                 | Post attitude     | -7.067  | -11.789 | 9.641    |
| Y               | on-board attitude | -9.881  | -16.635 | 14.210   |
|                 | Post attitude     | -0.219  | 3.246   | 2.007    |
| Z               | on-board attitude | 22.075  | 26.888  | 24.970   |
|                 | Post attitude     | 2.983   | 7.644   | 5.949    |

Tab 1. Position accuracy comparison (Earth Centered Earth Fixed)

As shown in table 1 above, it indicates obviously the positioning accuracy using post-attitude is higher than that using on-board attitude except the in x axis direction after geometric calibration. Especially, the error of elevation related to attitude accuracy has improved significantly. It demonstrates the post-processing attitude accuracy is better than the on-board attitude accuracy, and it meets requirements of the mapping production accuracy.

## 4. CONCLUSION

For the characteristic that real-time download raw attitude measurement data of ZY-3 satellite, post-UKF method was proposed and a comprehensive attitude post-processing strategy was realized in this paper, which achieved the high-precision data process of star tracker/gyro. The strategy proved its effectiveness by attitude comparison and ground verification. Meanwhile, post-processing attitude result was slightly better than the on-board attitude accuracy according to experimental verification results. It can be used in production of domestic high resolution satellite data, and provide reliability for geometric positioning.

Since the ground control data is limit, the selected two images have short time span, so the advantage of post-attitude is not obvious compared with on-board attitude, and the control data crossing long strips are required to further verify. In addition, the other combinations of star trackers and gyro also can be processed and contrastive analyzed

## 5. ACKNOWLEDGEMENT

This work is under the supporting of the Natural Science Foundation of China Grant (41301525) and state science and technology support program (2011BAB01B02).

Control Conference, Anchorage, USA, and 4555-4559.

[2]. Julier, S. J., Uhlmann, J. K., 1997. A New Extension of the Kalman Filter to Nonlinear Systems.

- In *Proc. of AeroSense: The 11th Int. Symp. on Aerospace/Defence Sensing, Simulation and Controls*.
- [3]. Van der Merwe, R., Wan E.A., 2001. Efficient Derivative-Free Kalman Filters for online Learning, In European Symposium on Artificial Neural Networks (ESANN), Bruges, Belgium.
- [4]. Matthew C. Vandyke, Jana L. Schwartz, Christopher D., 2004. Hall Unscented Kalman Filtering for Spacecraft Attitude State and Parameter Estimation, AAS-04-115. [www.dept.aoe.vt.edu/~cdhall/papers/AAS04-115.pdf](http://www.dept.aoe.vt.edu/~cdhall/papers/AAS04-115.pdf).
- [5]. Iwata Takanori, 2009. Precision attitude and position determination for Advanced Land Observing Satellite (ALOS). Proc. of SPIE Vol 5659:34-50.
- [6]. Takanori Iwata, Tetsuo Kawahara, 2007. Precision attitude determination for the advanced land observing satellite (ALOS): Design, Verification, and on-orbit calibration.
- [7]. J. Grodecki and G. Dial., 2001. IKONOS Geometric Accuracy. Proceedings of Joint Workshop of ISPRS Working Groups I/2, I/5 and IV/7 on High Resolution Mapping from Space
- [8]. David Mulawa, 2004. On-Orbit Geometric Calibration of the OrbView-3 High Resolution Imaging Satellite, Proceedings of ISPRS 2004, Istanbul, Turkey, July 12-23, 2004, URL: <http://www.isprs.org/proceedings/XXXV/congress/comm1/papers/1.pdf>.
- [9]. Landsat 7 Image Assessment System (IAS) Geometric Algorithm Theoretical Basis Document, Department of the Interior U.S. Geological Survey, LS-IAS-01, Version 1.0, [http://landsat.usgs.gov/documents/LS-IAS-01\\_Geometric\\_ATBD.pdf](http://landsat.usgs.gov/documents/LS-IAS-01_Geometric_ATBD.pdf).